

Hyperuniformity of quasiperiodic tilings generated by continued fractions

Mario Lázaro^{a,b,*}, Luis M. García-Raffi^b

^a*Department of Continuum Mechanics and Theory of Structures*

^b*Instituto Universitario de Matemática Pura y Aplicada
Universitat Politècnica de València (Spain)*

Abstract

Hyperuniformity is a property of certain heterogeneous media in which density fluctuations in the long wavelength range decay to zero. In reciprocal space this behavior translates into a decay of Fourier intensities in the range near small wavenumbers. In this paper quasiperiodic tilings constructed by word concatenation are under study. The lattice is generated from a parameter given by its continued fraction so that quasiperiodicity emerges for infinite when irrational generators are into consideration. Numerical simulations show a quite regular quadratic decay of Fourier intensities, regardless of the number considered for the generator parameter, which leads us to formulate the hypothesis that this type of media is strongly hyperuniform of order 3. Theoretical derivations show that the density fluctuations scale in the same proportion as the wavenumbers. Furthermore, it is rigorously proved that the structure factor decays around the origin according to the pattern $S(k) \sim k^4$. This result is validated with several numerical examples with different generating continued fractions.

Keywords:

hyperuniformity, quasiperiodic tilings, continued fractions, structure factor, Fourier intensities, reciprocal space

1. Introduction

Hyperuniformity is a property of a spatial distribution in which there are fewer density fluctuations at long length scales compared to a random distribution with the same number of points. In other words, hyperuniform systems have a more ordered structure than a typical random system, while still being statistically homogeneous. Quasicrystals (as Crystals) are hyperuniform [1]. For hyperuniform lattices, the structure factor $S(k)$ is a smooth function that tends to zero as the wavenumber k tends to zero following a power law, according to the equation

$$S(k) \sim k^\gamma \quad (1)$$

A consistent approach to standard cases characterized by smooth $S(k)$ and quasicrystals with dense but discontinuous $S(k)$ in 1D can be achieved by defining γ based on the integrated Fourier intensity

$$Z(k) = 2 \int_0^k S(\kappa) d\kappa \quad (2)$$

The integral is multiplied by 2 to be consistent with the definition for higher dimensions, where κ is viewed as a radial coordinate. For quasiperiodic lattices, $Z(k)$ is monotonically increasing and for k sufficiently small it can be plotted as bounded between to power-law curves verifying that

$$d_1 k^{\gamma+1} < Z(k) < d_2 k^{\gamma+1} \quad (3)$$

*Corresponding author. Tel +34 963877000 (Ext. 76732), malana@upv.es

for some constant coefficients d_1 and d_2 and for some γ . In such case γ is said to be order of hyperuniformity and the cumulative intensity function obeys a power law of order $1 + \gamma$, which is symbolized as

$$Z(k) \sim k^{\gamma+1}, \quad \text{as } k \rightarrow 0$$

Another measure of hyperuniformity is given by the local number variance of particles within a window of radius R (an interval of length $2R$ in the 1D case), denoted by $\sigma^2(R)$ (order metric context). If its growth is more slowly than the window volume (proportional to R in 1D) in the large- R limit, the system is hyperuniform. For any 1D system the scaling of $\sigma^2(R)$ for large R is determined by γ as follows: (class I, $\gamma > 1$) strongly hyperuniform, (class II, $\gamma = 1$) logarithmic hyperuniform and (class III, $0 < \gamma < 1$) weakly hyperuniform. Finally, for $\gamma < 0$ we have the anti-hyperuniform class [2].

In recent years, there has been significant research interest in hyperuniformity in quasiperiodic tilings, which are complex arrangements of tiles with long-range order but no translational symmetry. Studies have shown that certain types of quasiperiodic tilings exhibit hyperuniformity [2, 3], which has important implications for the physical and mechanical properties of these materials. Since hyperuniformity directly invokes particle order in the long wavelength range, the study of tile density depends on the generation pattern of these lattices. Thus, Orğuz et al. [3] have studied the hyperuniformity order in quasiperiodic lattices generated by projection, showing that it depends on the type of strip used. The so-called ideal strips result in hyperuniformity exponents of $\gamma = 3$. Other important case of quasiperiodic 1D structures are those generated by substitution rules (or inflation rules). It turns out that there is a strong relationship between the scaling in Fourier intensities and density fluctuations in the limit tiling [4–6]. In particular, the eigenvalues of the substitution matrix play an important role in this relationship [7, 8]. The hyperuniformity of substitution quasiperiodic tilings has been discussed in detail in the reference [9], showing that the power-decay law of Fourier intensities strongly depends on the nature of the substitution matrix. Fuchs et. al. [?] have found log-periodic oscillations of the broadening of Landau levels in the presence of a potential with discrete scale invariance, determining exactly the hyperuniformity exponent and the period of such oscillations.

In this paper we present a comprehensive analysis of the hyperuniformity of quasi-periodic lattices based on word concatenation and generated by continuous fractions. By making use of the recursive nature of these systems, iterative expressions for both Fourier intensities and density fluctuations can be obtained analytically. Both are a function of the different coefficients that form the continued fraction. Analytical expressions for the decreasing pattern of Fourier intensities with wavenumbers for quasiperiodic tilings generated by the so-called Metallic means and by periodic continued fractions are derived in detail, showing good agreement with the numerical examples. Furthermore, it is also proved that the global hyperuniform behavior of the structure factor is $S(k) \sim k^4$.

2. Quasiperiodic tilings generated by concatenation

Let us consider two segments (tiles) of lengths A and B and a real number $\alpha \in \mathbb{R}$ defined in the range $0 < \alpha \leq 1$. Let the sequence $[0; a_1, \dots, a_n]$ be the continuous fraction of α , namely we can write

$$\alpha = [0; a_1, \dots, a_n] = \frac{1}{a_1 + \frac{1}{\dots + \frac{1}{a_{n-1} + \frac{1}{a_n}}}} \quad (4)$$

where $a_j > 0$, for $j \geq 1$, are positive integer numbers.

Using the terms of this sequence, a word can be formed from the alphabet $\{A, B\}$ by concatenation. The recursive formula is defined as

$$\begin{aligned}\mathcal{W}_j &= \mathcal{W}_{j-1}^{a_j} \mathcal{W}_{j-2}, \quad 1 \leq j \leq n \\ \mathcal{W}_{-1} &= A, \quad \mathcal{W}_0 = B\end{aligned}\tag{5}$$

where both the exponent and the product must be understood as concatenations, for instance $A^3(B^2A) = AAABBA$. The parameter α plays the role of *generation parameter* of the quasiperiodic tiling. From the definition given above, if α is a rational number the word \mathcal{W}_n corresponds to the last iteration. The infinite word emerges as the periodic concatenation of \mathcal{W}_n . Otherwise, if α is irrational, then it is known that the sequence $\{a_n\}$ becomes infinite and the associated word has a purely quasiperiodic pattern given by the limit $\lim_{n \rightarrow \infty} \mathcal{W}_n$. We will refer to the algorithm given by Eq. (5) as *concatenation algorithm*, since the words at each step arise from the concatenation of the previous ones. For instance, for $\alpha = 3/11 = [0; 3, 1, 2]$ the Fig. 1 shows the different words after each step and the final tiling \mathcal{W}_3 .

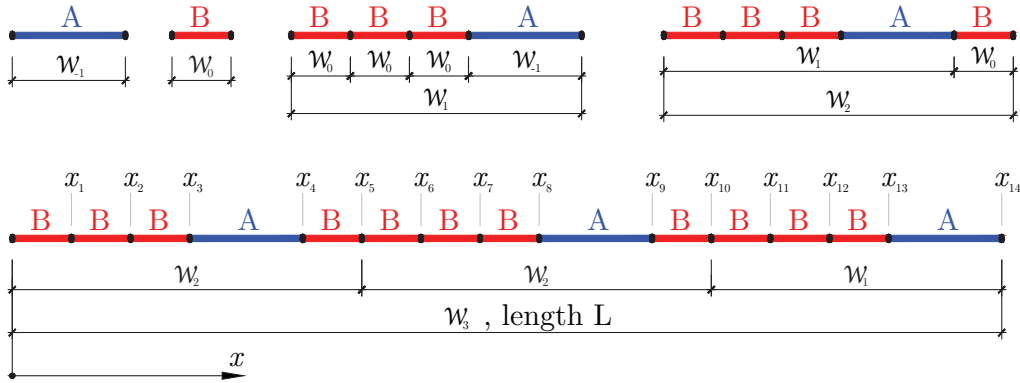


Figure 1: Tiling generation by concatenation for parameter $\alpha = 3/11 = [0; 3, 1, 2]$. Convergents are $\alpha_j = \{1/3, 1/4, 3/11\}$. Numerators and denominators of convergents match with the step number of tiles of each type

The final goal is the word \mathcal{W}_n associated to the tiling generated by α . However, words of previous steps are somehow approximations. In particular, the number of symbols A and B at each step is given by the sequences u_j and v_j respectively, defined recursively as

$$u_j = a_j u_{j-1} + u_{j-2}, \quad u_{-1} = 1, \quad u_0 = 0\tag{6}$$

$$v_j = a_j v_{j-1} + v_{j-2}, \quad v_{-1} = 0, \quad v_0 = 1\tag{7}$$

Both u_j and v_j are numerator and denominator of the j th convergent $\alpha_j = u_j/v_j$ [10], with $\alpha = \alpha_n$. Thus

$$\frac{u_1}{v_1} = \frac{1}{a_1}, \quad \frac{u_2}{v_2} = \frac{1}{a_1 + \frac{1}{a_2}}, \quad \dots, \quad \frac{u_n}{v_n} = \frac{1}{a_1 + \frac{1}{a_2 + \frac{1}{a_3 + \frac{1}{\dots + \frac{1}{a_{n-1} + \frac{1}{a_n}}}}}}\tag{8}$$

Moreover, for two consecutive steps the following identity holds [11]

$$v_j u_{j-1} - u_j v_{j-1} = (-1)^j, \quad 1 \leq j \leq n\tag{9}$$

which leads to the known distance between two consecutive convergents

$$\alpha_{j-1} - \alpha_j = \frac{(-1)^j}{v_j v_{j-1}}$$

For the tiling associated to the word \mathcal{W}_j , both the total number of points and tiling length are then $N_j = u_j + v_j$ and $L_j = u_j A + v_j B$ respectively, which can also be determined recursively as

$$\begin{aligned} N_j &= a_j N_{j-1} + N_{j-2}, & 1 \leq j \leq n, & & N_{-1} = 1, & & N_0 = 1 \\ L_j &= a_j L_{j-1} + L_{j-2}, & 1 \leq j \leq n, & & L_{-1} = A, & & L_0 = B \end{aligned} \quad (10)$$

Therefore, the total number of points $N = N_n$ and the final length of the tiling $L = L_n$ are

$$N = (1 + \alpha) v_n, \quad L = A u_n + B v_n = (B + \alpha A) v_n \quad (11)$$

3. Properties of the Structure Factor

The pattern of points generated by the Sturmian word can be considered as a distribution of local heterogeneities. Thus, the density of the medium generated after n iterations of Eq. (5) can be written in terms of Dirac-delta functions as

$$g(x) = \sum_{j=1}^N \delta(x - x_j) \quad (12)$$

and its corresponding Fourier series representation leads to

$$g(x) = \sum_{m=-\infty}^{\infty} \hat{g}(k_m) e^{ik_m x} \quad (13)$$

where the Fourier coefficients are

$$\hat{g}(k_m) = \frac{1}{L} \int_{x=0}^L g(x) e^{-ik_m x} dx, \quad k_m = \frac{2\pi m}{L}, \quad m = 0, \pm 1, \pm 2, \dots \quad (14)$$

The sequence $\{k_m\}$ represent the reciprocal space positions and according to Eq. (12) the integral is

$$\int_{x=0}^L g(x) e^{-ik x} dx = \sum_{j=1}^N e^{-ik x_j} \quad (15)$$

In general, evaluation of Eq. (15) requires in first place the concatenation of the complete word \mathcal{W}_n , and secondly the determination the N real space coordinates x_j , $1 \leq j \leq N$. Taking advantage of the recursive formation of the words, we propose a new iterative approach to find the expression of Eq. (15), avoiding the computation of the N coordinates x_j . This procedure is suitable for quasiperiodic 1D lattices generated by concatenation and it can result useful, especially when handling large systems, which is necessary to simulate aperiodic media.

Consider any word \mathcal{U} formed by U symbols taken from the alphabet $\{A,B\}$, and real space positions of points given by $\{x_j, 1 \leq j \leq U\}$. Let us define

$$\mathcal{F}\{\mathcal{U}; k\} = \sum_{j=1}^U e^{-ik x_j} \quad (16)$$

As long as there is no room for confusion, we will henceforth refer as Fourier coefficients to those obtained by the above expression (16). We are interested in evaluating Eq. (16) for words generated by concatenation. Thus, let us consider \mathcal{U} and \mathcal{V} two arbitrary words formed with symbols taken from the alphabet $\{A,B\}$, with lengths l_u and l_v and with a total number of symbols equal to U and V , respectively. Let us consider

$\{x_j, 1 \leq j \leq U\}$ and $\{y_j, 1 \leq j \leq V\}$ to be the local positions of tiles for both tilings respectively, verifying that

$$\mathcal{F}\{\mathcal{U}; k\} = \sum_{j=1}^U e^{-ikx_j} \quad , \quad \mathcal{F}\{\mathcal{V}; k\} = \sum_{j=1}^V e^{-iky_j} \quad (17)$$

Then the word \mathcal{UV} obtained by concatenation has a length $l_u + l_v$ and $U + V$ particles whose coordinates respect to the origin of the concatenated word are

$$\{x_1, \dots, x_U, l_u + y_1, \dots, l_u + y_V\} \quad (18)$$

The Fourier coefficients of the new tiling is

$$\mathcal{F}\{\mathcal{UV}; k\} = \mathcal{F}\{\mathcal{U}; k\} + e^{-ikl_u} \mathcal{F}\{\mathcal{V}; k\} \quad (19)$$

Given any integer number m and using the induction principle from this result it is straightforward that

$$\begin{aligned} \mathcal{F}\{\mathcal{U}^m; k\} &= \left(1 + e^{-ikl_u} + e^{-i2kl_u} + \dots + e^{-i(m-1)kl_u}\right) \mathcal{F}\{\mathcal{U}; k\} \\ &\equiv \mathcal{P}(m, l_u; k) \mathcal{F}\{\mathcal{U}; k\} \end{aligned} \quad (20)$$

where

$$\mathcal{P}(m, l; k) = 1 + e^{-ikl} + e^{-i2kl} + \dots + e^{-i(m-1)kl} = \frac{1 - e^{-ikml}}{1 - e^{-ikl}} \quad (21)$$

stands for the Fourier intensities of a periodic tiling of m particles with separation l , that is with coordinates $\{0, l, 2l, \dots, (m-1)l\}$. Making use of the properties given by Eqs. (19) and (20) and denoting by $\mathcal{H}_j(k) = \mathcal{F}\{\mathcal{W}_j; k\}$ for $1 \leq j \leq n$, it yields

$$\begin{aligned} \mathcal{H}_j(k) &= \mathcal{F}\{\mathcal{W}_{j-1}^{a_j} \mathcal{W}_{j-2}; k\} \\ &= \mathcal{F}\{\mathcal{W}_{j-1}^{a_j}; k\} + e^{-ikL_{j-1}} \mathcal{F}\{\mathcal{W}_{j-2}; k\} \\ &= \mathcal{P}(a_j, L_{j-1}; k) \mathcal{H}_{j-1}(k) + e^{-ikL_{j-1}} \mathcal{H}_{j-2}(k) \quad , \quad 1 \leq j \leq n \\ \mathcal{H}_{-1}(k) &= e^{-ikA} \\ \mathcal{H}_0(k) &= e^{-ikB} \end{aligned} \quad (22)$$

As this new recursive scheme shows, the Fourier coefficients can be obtained just iterating n times the Eq. (22). Thus, it is not necessary to compute the N coordinates of the whole medium, something remarkable from a computational point of view, because in general $N \gg n$.

The Fourier coefficients define the properties of the medium in reciprocal space. Media studied in this paper have a discrete distribution of reciprocal space positions k given by $k = 2\pi m/L$, with $m = 0, \pm 1, \pm 2, \dots$. If A/B is rational, any system obtained by a finite number of interactions n will be periodic having a bounded band of information in the reciprocal space. That is, the distribution of Fourier amplitudes will be periodic. Given a medium of N particles within a length L , let us see the period of this distribution. Indeed, the final expression of Fourier coefficients is $\sum \exp\{ikx_j\}$. Assuming $A/B = \theta_A/\theta_B$ is the irreducible fraction of the tiles lengths ratio, then there exist a value of k for which the Fourier coefficients is periodic. That period corresponds to

$$K_P = \frac{2\pi\theta_B}{B} = \frac{2\pi\theta_A}{A} \quad (23)$$

If A/B is irrational, numerator and denominator of the rational approximation θ_A/θ_B approaches to infinite making also aperiodic the spectrum in the reciprocal space. It results of interest the fact the period derived in Eq. (23) is independent of the iterations of Eq. (22), so that $\mathcal{H}_j(k)$, $j \geq 1$ are periodic with period $k = K_P$.

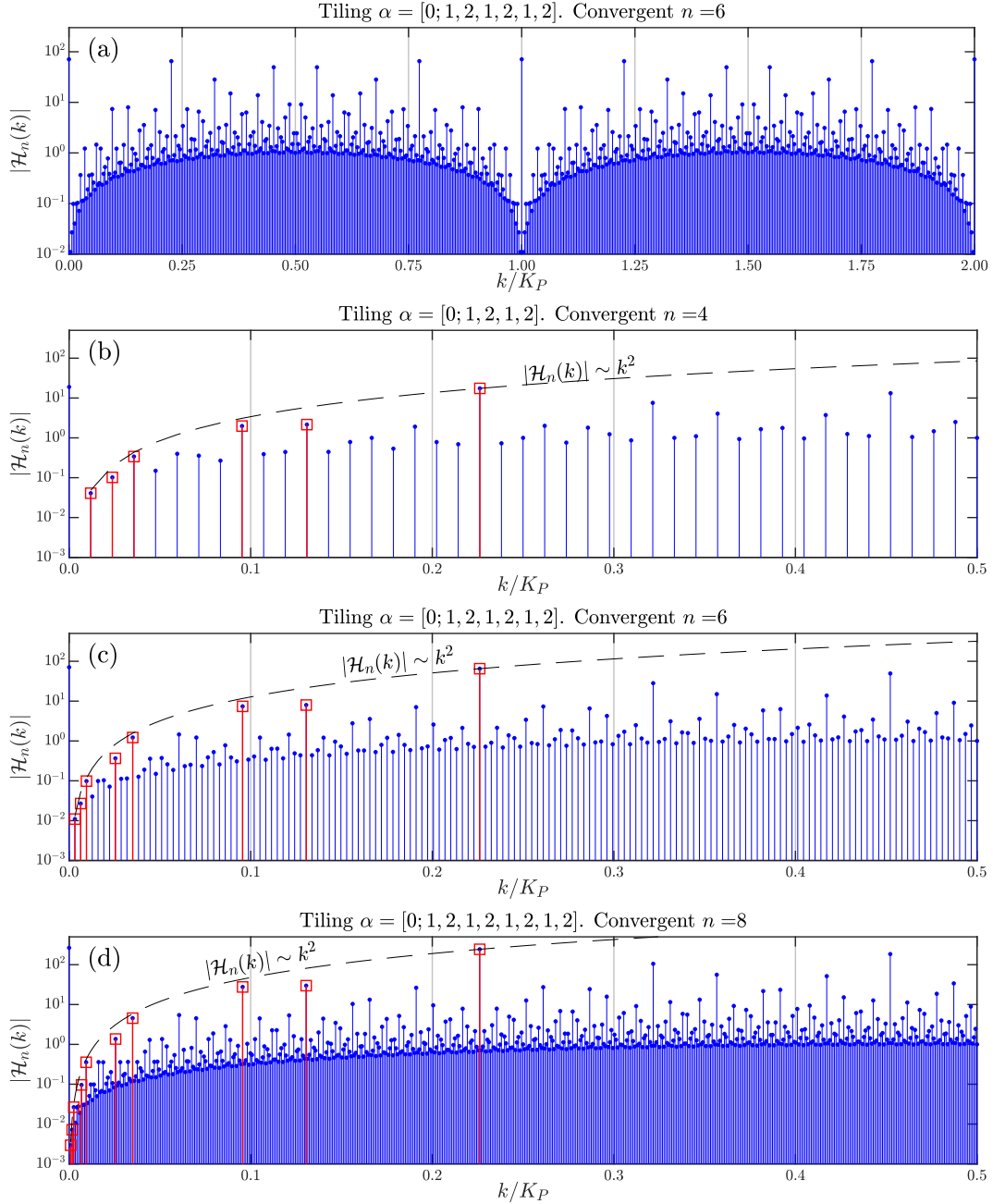


Figure 2: Fourier magnitudes for the tiling associated to $\alpha = \sqrt{3} - 1 = [0; 1, 2, 1, 2, \dots]$. (a) Fourier magnitudes of the 6th iteration in the range $0 \leq k \leq 2K_P$. In plots (b), (c) and (d): Fourier magnitudes of the 4th, 6th and 8th iterations respectively in the range $0 \leq k \leq K_P/2$. Blue dots: complete spectrum of Fourier magnitudes. Red squares: Fourier magnitudes at the sequence of dominant wavenumbers $\{k_\nu\}_{\nu=-1}^n$. Dashed lines: curve proportional to k^2

Let us illustrate these results graphically with a numerical example. Let us consider the tiling associated to the parameter $\alpha = \sqrt{3} - 1 = [0; 1, 2, 1, 2, \dots] = 0.7320508\dots$ with tiles lengths $A = 1.25$ and $B = 1.00$ (units of length), so that $\theta_A = 5$ and $\theta_B = 4$. According to Eq. (23) the spectrum of the Fourier coefficients in the reciprocal space is periodic with period $K_P = 8\pi$. The magnitudes of the Fourier coefficients

corresponding to the 6th convergent $\alpha_6 = [0; 1, 2, 1, 2, 1, 2] = 0.73170$ are shown in Fig. 2(a). The range has been extended to $k/K_P = 2$ to show the periodicity due to the rational nature of A/B . However, within the range $k/K_P = [0, 1]$ the self-similarity of the patterns at different scales, typical of quasi-periodic structures, is observed. In Figs.2(b), 2(c) and 2(d) the image has been enlarged in the range $k/K_P = [0, 0.5]$. The three plots represent respectively the Fourier intensities for convergents $n = 4$, $n = 6$ and $n = 8$. It is observed that the limit quasiperiodic tiling present a decreasing intensities as the wavenumbers approach to zero ($k \rightarrow 0$), showing evidences of hyperuniform behavior. Moreover, one particular sequence of Bragg peaks, represented in red, show a more pronounced pattern, proportional to k^2 . In the next point, the sequence of these characteristic wavenumbers (drawn in red color in Fig. 2) will be derived.

4. Sequence of dominant wavenumbers

Consider the tiling generated by $\alpha = [0; a_1, \dots, a_n] = u_n/v_n$, with length $L = L_n = Au_n + Bv_n$. For each j with $0 \leq j \leq n$ we can define the parameter σ_j obtained as the remaining continued fraction after truncation of α up to position j , i.e.

$$\sigma_j = [0; a_{j+1}, a_{j+2}, \dots, a_n] = \frac{1}{a_{j+1} + \frac{1}{a_{j+2} + \frac{1}{\ddots + \frac{1}{a_{n-1} + \frac{1}{a_n}}}}} \quad (24)$$

with $\sigma_0 = \alpha$ and $\sigma_n = 0$. The number σ_j plays a key role in the subsequent developments, specially in the computation of the so-called density fluctuations of the tiling. So, it is interesting to derive two different ways of expressing its value, additionally to the continued fraction given by Eq. (24). First, using the properties of continued fraction [11], it can be established that

$$\alpha = [0; a_1, \dots, a_j, a_{j+1}, \dots, a_n] = \frac{(a_j + \sigma_j)u_{j-1} + u_{j-2}}{(a_j + \sigma_j)v_{j-1} + v_{j-2}} = \frac{u_j + \sigma_j u_{j-1}}{v_j + \sigma_j v_{j-1}} \quad (25)$$

and solving for σ_j

$$\sigma_j = -\frac{\alpha - \alpha_j}{\alpha - \alpha_{j-1}} \frac{v_j}{v_{j-1}} \quad (26)$$

Secondly, let us express σ_j in form of irreducible fraction. For that, we invoke the following decreasing sequence

$$\xi_j = a_j \xi_{j-1} + \xi_{j-2}, \quad \xi_{-1} = -v_n, \quad \xi_0 = u_n \quad (27)$$

with general term [10]

$$\xi_j = v_n v_j (\alpha - \alpha_j) \quad (28)$$

Taking into account Eqs (26) (28), the sequence $\{\xi_j\}$ presents alternating sign and approaches to zero around the limit value α . Moreover, in general

$$\sigma_j = -\frac{\xi_j}{\xi_{j-1}}, \quad 0 \leq j \leq n \quad (29)$$

Since the initial values are $\xi_{-1} = -v_n$, $\xi_0 = u_n$, then ξ_j will be negative for odd indexes and positive for even ones. Based on this, the sequence $c_j = (-1)^{j-1} \xi_{j-1}$ for $0 \leq j \leq n+1$, is formed by positive integer numbers and decreasing order from $c_0 = v_n$ up to $c_n = 1$ and $c_{n+1} = 0$. The recursive relationship between sequences $\{c_j\}$ and $\{\sigma_j\}$ is then straightforward and given by

$$c_{j+1} = \sigma_j c_j, \quad 0 \leq j \leq n \quad (30)$$

Such set of numbers $\{c_j\}$ so formed will be used as basis to build a sequence of wavenumbers associated to the tiling α_n . This sequence will be of special importance in the forthcoming developments and it is defined as

$$k_\nu = \frac{2\pi}{L_n} c_\nu, \quad 0 \leq \nu \leq n \quad (31)$$

Additionally, the term associated to $\nu = -1$ as $k_{-1} = 2\pi N_n/L_n$ will be added at the beginning of the sequence. It should be pointed out that this is a sequence of positive and decreasing numbers, since according to Eq. (30) each term is obtained by multiplying the previous one by σ_j which is less than the unity. In Fig. 2(b), (c) and (d) the Fourier intensities at these $n+2$ coordinates have been highlighted in red color. As observed, the number of terms of this sequence increases as the corresponding convergent α_n does. The Fourier intensities at these locations reveal strong periodic patterns in direct space, closely related to the formation of the tiling. Taking a closer look at these wavenumbers for the three systems shown ($n = 4$, $n = 6$ and $n = 8$), it results clear that their positions fit quite accurately as higher convergents are considered. Each column of Table 1 shows the numerical results of the $n+2$ wavenumbers k_ν/K_P , $-1 \leq \nu \leq n$ associated to each generating parameter α_n (including the added wavenumber for $\nu = -1$, introduced above). If, on the other side, we focus on a row, say the ν -th one, the different values represent how changes the value of k_ν as the tiling increases. Here is where the results of the table become interesting. Thus, let us consider for instance the values of the wavenumbers k_0 ($\nu = 0$), which are listed in the second row. As shown above, $c_0 = v_n$, yielding

$$k_0 = \left\{ \frac{2\pi v_1}{L_1}, \frac{2\pi v_2}{L_2}, \dots, \frac{2\pi v_8}{L_8} \right\} = \left\{ \frac{2\pi}{B + A\alpha_1}, \frac{2\pi}{B + A\alpha_2}, \dots, \frac{2\pi}{B + A\alpha_8} \right\} \quad (32)$$

In general we can denote by $k_0(\alpha_n) = 2\pi/(B + \alpha_n A)$ to the wavenumber for $\nu = 0$ calculated for the tiling $\alpha_n = [0; a_1, \dots, a_n]$. From the definition of convergents, we can conclude that if $n \gg 1$, then it is expected that

$$k_0(\alpha_n) \approx k_0(\alpha_{n+1}) \approx k_0(\alpha_{n+2}) \approx \dots \quad (33)$$

After a quick inspection of the numerical values shown in the second row of Table 1, we note that the first 4 decimal positions of k_0 stabilize from the 6th convergent ($n = 6$) onwards. In general, let us prove that

ν	Tiling, α_n							
	$n = 1$	$n = 2$	$n = 3$	$n = 4$	$n = 5$	$n = 6$	$n = 7$	$n = 8$
k_{-1}	0.222222	0.227273	0.225806	0.226190	0.226087	0.226115	0.226107	0.226109
k_0	0.111111	0.136364	0.129032	0.130952	0.130435	0.130573	0.130536	0.130546
k_1	0.111111	0.090909	0.096774	0.095238	0.095652	0.095541	0.095571	0.095563
k_2	-	0.045455	0.032258	0.035714	0.034783	0.035032	0.034965	0.034983
k_3	-	-	0.032258	0.023810	0.026087	0.025478	0.025641	0.025597
k_4	-	-	-	0.011905	0.008696	0.009554	0.009324	0.009386
k_5	-	-	-	-	0.008696	0.006369	0.006993	0.006826
k_6	-	-	-	-	-	0.003185	0.002331	0.002560
k_7	-	-	-	-	-	-	0.002331	0.001706
k_8	-	-	-	-	-	-	-	0.000853

Table 1: Each row shows the value of k_ν/K_P for different tilings α_n , with $n \geq \nu$, generated by the convergents of the number $[0; 1, 2, 1, 2, 1, 2, \dots]$. The theoretical results show that after a few iterations, the value of k_ν stabilizes showing that $k_\nu(\alpha_{n-1}) \approx k_\nu(\alpha_n)$ for $n \gg \nu$.

the following expression approximately holds provided that $n \gg \nu \geq -1$,

$$\frac{k_\nu(\alpha_{n-1})}{k_\nu(\alpha_n)} \approx 1 \quad (34)$$

Indeed, from of Eqs. (30) and (31) it can be established that

$$\begin{aligned}
k_\nu(\alpha_n) &= \sigma_{\nu-1}(\alpha_n) k_{\nu-1}(\alpha_n) = \sigma_{\nu-1}(\alpha_n) \sigma_{\nu-2}(\alpha_n) k_{\nu-2}(\alpha_n) \\
&= \cdots = \sigma_{\nu-1}(\alpha_n) \sigma_{\nu-2}(\alpha_n) \cdots \sigma_0(\alpha_n) k_0(\alpha_n) \quad (35)
\end{aligned}$$

where the dependence on the associated convergent α_n has been highlighted using notation $k_\nu(\bullet)$ and $\sigma_\nu(\bullet)$. This detail in notation is important at this stage since the quotient of Eq.(34) is the result of evaluating Eq. (35) for two consecutive convergents, α_{n-1} and α_n , indeed

$$\begin{aligned}
\frac{k_\nu(\alpha_{n-1})}{k_\nu(\alpha_n)} &= \frac{\sigma_{\nu-1}(\alpha_{n-1})}{\sigma_{\nu-1}(\alpha_n)} \cdots \frac{\sigma_1(\alpha_{n-1})}{\sigma_1(\alpha_n)} \frac{\sigma_0(\alpha_{n-1})}{\sigma_0(\alpha_n)} \frac{k_0(\alpha_{n-1})}{k_0(\alpha_n)} \\
&= \frac{[0; a_\nu, a_{\nu+1}, \dots, a_{n-1}]}{[0; a_\nu, a_{\nu+1}, \dots, a_n]} \cdots \frac{[0; a_2, \dots, a_{n-1}]}{[0; a_2, \dots, a_n]} \frac{[0; a_1, \dots, a_{n-1}]}{[0; a_1, \dots, a_n]} \frac{B + A\alpha_n}{B + A\alpha_{n-1}} \\
&\approx 1 \times \cdots \times 1 \times 1 \approx 1, \quad n \gg \nu \geq 1 \quad (36)
\end{aligned}$$

The values of each of the fractions $\sigma_j(\alpha_{n-1})/\sigma_j(\alpha_n)$ for $0 \leq j \leq \nu - 1$ are approximately the unity since it is assumed that $n \gg \nu \geq 1$. Moreover, for $\nu = -1$ and $\nu = 0$, it yields too

$$\begin{aligned}
\frac{k_{-1}(\alpha_{n-1})}{k_{-1}(\alpha_n)} &= \frac{2\pi N_{n-1}}{L_{n-1}} \frac{L_n}{2\pi N_n} = \frac{1 + \alpha_{n-1}}{1 + \alpha_n} \frac{B + A\alpha_n}{B + A\alpha_{n-1}} \approx 1 \\
\frac{k_0(\alpha_{n-1})}{k_0(\alpha_n)} &= \frac{2\pi v_{n-1}}{L_{n-1}} \frac{L_n}{2\pi v_n} = \frac{B + A\alpha_n}{B + A\alpha_{n-1}} \approx 1 \quad (37)
\end{aligned}$$

These Bragg peaks in reciprocal space have consequences on the behavior of the medium in the long wavelength range. The recursive expression of the Fourier intensities will help to show why this sequence of wavenumbers have dominant magnitudes. Indeed, using Eq. (22), the Fourier magnitude associated to the tiling α_n at the wavenumbers $k = k_\nu(\alpha_n) \approx k_\nu(\alpha_{n-1})$ are

$$\begin{aligned}
\mathcal{H}_n[k_\nu(\alpha_n)] &= \mathcal{P}[a_n, L_{n-1}; k_\nu(\alpha_n)] \mathcal{H}_{n-1}[k_\nu(\alpha_n)] + e^{-i k_\nu(\alpha_n) L_{n-1}} \mathcal{H}_{n-2}[k_\nu(\alpha_n)] \\
&\approx \mathcal{P}[a_n, L_{n-1}; k_\nu(\alpha_{n-1})] \mathcal{H}_{n-1}[k_\nu(\alpha_{n-1})] + e^{-i k_\nu(\alpha_{n-1}) L_{n-1}} \mathcal{H}_{n-2}[k_\nu(\alpha_{n-1})] \\
&= a_n \mathcal{H}_{n-1}[k_\nu(\alpha_{n-1})] + \mathcal{H}_{n-2}[k_\nu(\alpha_{n-1})], \quad \text{for } n \gg \nu \geq -1 \quad (38)
\end{aligned}$$

$$(39)$$

where the last step $\mathcal{P}[a_n, L_{n-1}; k_\nu(\alpha_{n-1})] = a_n$ holds because $\mathcal{P}(m, l; k) = m$ when $kl/2\pi$ is a integer number. Following the recursive scheme and, as long as j is sufficiently far from ν , we can approximate

$$\begin{aligned}
\mathcal{P}[a_j, L_{j-1}, k_\nu(\alpha_j)] &\approx \mathcal{P}[a_j, L_{j-1}, k_\nu(\alpha_{j-1})] = a_j \\
e^{-i k_\nu(\alpha_j) L_{j-1}} &\approx e^{-i k_\nu(\alpha_{j-1}) L_{j-1}} = 1, \quad n \geq j \gg \nu \quad (40)
\end{aligned}$$

i.e. they take their maximum values. The Fourier intensities $\mathcal{H}_n(k)$ at wavenumbers $k = k_\nu$, with $n \gg \nu$, result maximized with respect to other wavenumbers in their neighborhood. This explains why their intensities are several orders of magnitude larger than the rest. Furthermore, in Fig. 2, it can be observed that the law of the form $|\mathcal{H}_n(k)| \sim k^2$, seems to fit more accurately at the Bragg peaks of the sequence $\{k_\nu\}$.

The approximation of Eqs.(36) and (37) gets worse as the value of $k_\nu(\alpha_{n-1})$ differs from $k_\nu(\alpha_n)$, which becomes evident as ν gets closer to n . However, recall we can make n as large as we want for a pure quasiperiodic tiling generated by an infinite continued fraction. Thus, the Fourier intensities at these Bragg peaks at the sequence $\{k_\nu\}$ decays towards $k \rightarrow 0$ following a pattern stronger than the linear one. In fact, we will see in the next section that, under certain assumptions tested in previous works we can predict analytically the Fourier intensities in this sequence of wavenumbers, which will be called *sequence of dominant wavenumbers*.

5. Hyperuniformity exponent

It is well known that the order of hyperuniformity of a medium in reciprocal space is closely related to the limiting values of density fluctuations in the physical space. In the particular case of quasiperiodic media generated by substitution, it has been observed that the hyperuniformity and the limit density fluctuations are close related [2] and in turn these latter are proportional to the ratio of the two eigenvalues of the substitution matrix. Our goal is to extend these results to the family of quasiperiodic systems generated by concatenation of words using a continued fraction, as shown in Eq. (5). Let us consider a tiling based on the convergent $\alpha = [0; a_1 \dots, a_n]$, with $n \gg 1$. As the words $\{\mathcal{W}_j, 1 \leq j \leq n\}$ are generated, both the number of tiles N_j and the length of the tiling L_j become larger. The density of points associated to the j th convergent $\alpha_j = [0; a_1, \dots, a_j] = u_j/v_j$ can be determined as $\rho_j = N_j/L_j$. From Eqs. (10) and (11) and after j iterations, the density of points yields

$$\rho_j = \frac{N_j}{L_j} = \frac{u_j + v_j}{Au_j + Bv_j} = \frac{1 + \alpha_j}{B + \alpha_j A} \quad (41)$$

Denoting by $\bar{\rho} = N/L = (1 + \alpha)/(B + \alpha A)$ to the limit density of tile vertices, then we can write $\rho_j = \bar{\rho} + \delta\rho_j$, where $\delta\rho_j$ stands for the deviations respect to $\bar{\rho}$ and they are given by

$$\delta\rho_j = \frac{(A - B)(\alpha - \alpha_j)}{(B + \alpha_j A)(B + \alpha A)} \quad , \quad 1 \leq j \leq n \quad (42)$$

This relationship exhibits the decreasing amplitudes of density fluctuations for large scales, characteristic of hyperuniform structures. From Eq. (42), the ratio between density fluctuations for two consecutive iterations yields

$$\frac{\delta\rho_j}{\delta\rho_{j-1}} = \frac{\alpha - \alpha_j}{\alpha - \alpha_{j-1}} \frac{B + A\alpha_{j-1}}{B + A\alpha_j} \quad (43)$$

This expression reveals the close relationship between the ratio of density fluctuations and the parameter σ_j introduced in the previous section. Furthermore, using Eq. (26) we can rewrite the above equation as

$$\frac{\delta\rho_j}{\delta\rho_{j-1}} = -\sigma_j \tau_j \quad (44)$$

where the new parameter $\tau_j = L_{j-1}/L_j$ denotes the relationship between tiling lengths at two consecutive iterations. As shown in Eq. (10), the sequence of the tiling lengths obeys the recursive scheme given by $L_j = a_j L_{j-1} + L_{j-2}$. Therefore, the parameter τ_j can be expressed in other form as

$$\tau_j = \frac{L_{j-1}}{L_j} = \frac{1}{a_j + \frac{1}{a_{j-1} + \frac{1}{\dots + \frac{1}{a_1 + \frac{\theta_A}{\theta_B}}}}} = [0; a_j, a_{j-1}, \dots, a_1 + \theta_A/\theta_B] \quad (45)$$

Eq. (44) reveals that density fluctuations decay following an exponential-type law and alternating the corresponding sign around the average density. It is known that one-dimensional quasiperiodic media generated by substitution rules exhibit density fluctuations that depend on the eigenvalues of the substitution matrix [2]. Moreover, in such media it has been found [12, 13] that the Fourier intensities are scaled under the same pattern as the density fluctuations. Aperiodic tilings studied in this paper are built by means of word concatenation, governed by a generic continued fraction $[0; a_1, \dots, a_n]$. Thus, each new word depends on a new number a_j given by the continued fraction, making them of special nature. After the definition of the sequence of dominant wavenumbers, see Eqs. (30) and (31), and considering the derived expression for the density fluctuations ratio in Eq. (44), two major facts have been identified

- (i) According to Eq. (39), the Fourier intensities are maximized at the dominant wavenumber sequence $k_{\nu+1} = \sigma_\nu k_\nu$
- (ii) Ratio of two consecutive density fluctuations is proportional to the ratio between two consecutive dominant wavenumbers, i.e. $\frac{\delta\rho_\nu}{\delta\rho_{\nu-1}} = -\sigma_\nu \tau_\nu$

For the purposes of this section, we can ignore the subscript n since other convergents will not be of interest. Thus, for convenience in notation, let us denote as $H(k) = |\mathcal{H}_n(k)|$ to the magnitude of the Fourier intensity of tiling generated by $\alpha = [0, a_1, \dots, a_n]$ at wavenumber k . Assuming the hypothesis that Fourier intensities scales as the density fluctuations, we can establish the following relationship for each pair of consecutive wavenumbers within the sequence $\{k_\nu\}_{\nu=0}^{n-1}$

$$H(\sigma_\nu k_\nu) = \left| \frac{\delta\rho_\nu}{\delta\rho_{\nu-1}} \right| \cdot H(k_\nu) \quad (46)$$

Assuming a power law for the Fourier magnitudes, we find that

$$\frac{H(k_{\nu+1})}{H(k_\nu)} = \left(\frac{k_{\nu+1}}{k_\nu} \right)^{1+\log \tau_\nu / \log \sigma_\nu}, \quad 0 \leq \nu \leq n-1 \quad (47)$$

where both σ_ν and τ_ν can be written as the continued fractions

$$\begin{aligned} \tau_\nu &= [0; a_\nu, a_{\nu-1}, \dots, a_1 + \theta_A/\theta_B] \\ \sigma_\nu &= [0; a_{\nu+1}, a_{\nu+2}, \dots, a_n] \end{aligned} \quad (48)$$

Therefore, the structure factor decays with wavenumbers according to the law

$$\frac{S(k_{\nu+1})}{S(k_\nu)} = \left(\frac{k_{\nu+1}}{k_\nu} \right)^{2+2 \log \tau_\nu / \log \sigma_\nu}, \quad 0 \leq \nu \leq n-1 \quad (49)$$

As Eqs. (47) and (49) show, the scaling factor in the Fourier intensities is variable for each step depending on the continued fraction sequence $\{a_j, 1 \leq j \leq n\}$. Thus, new higher terms of the sequence $\{a_n\}$ provide information on successive scales in the large wavelength range, or in other words, in the different small scales in the reciprocal space, around $k \rightarrow 0$. Let us illustrate the proposed model of Eq. (47) with an example.

Let us consider for that the tiling generated by

$$\alpha = [0; 1, 8, 1, 8, 1, 8, 1, 8, 2, 2, 2, 2, \dots] \approx 0.8989789 \dots$$

The Fourier intensities can be determined using the recursive procedure proposed in Eq. (22) for each wavenumber $k = 2\pi m/L$, $m = 0, \pm 1, \pm 2, \dots$. They have been plotted in Fig. 3, highlighting in red color the Bragg peaks at the dominant wavenumbers $k_\nu = 2\pi c_\nu/L$, $0 \leq \nu \leq n$, defined in Eqs. (31). The first term of the sequence, for $\nu = 0$ is also the highest one, with value $k_0 = 2\pi v_n/L \approx 2\pi/(B + A\alpha)$. As the index ν increases in the range $0 \leq \nu \leq n$, the value of k_ν decays up to the last (and lowest) value $k_n = 2\pi/L$. The subsequent Fourier intensities $H(k_\nu)$ from $\nu = n-1$ up to $\nu = 0$ can be obtained recursively from the previous ones by means of proposed approach of Eq. (47), starting from $H(k_n)$. These values are shown with blue-dashed line shown in Fig. 3. The proposed method satisfactorily fits the exact results of the spectrum in the reciprocal space at the coordinates given by the dominant wavenumbers $\{k_\nu\}_{\nu=0}^n$. In order to obtain the Fig. 3, the 12th approximant of α ($n = 12$) has been considered. As known, the sequence k_ν follows the recursive scheme $k_{\nu+1} = \sigma_\nu k_\nu$. In the particular case of $\alpha = [0; 1, 8, 1, 8, 1, 8, 2, 2, 2, 2, 2]$, the sequence of numbers $\{\sigma_\nu\}$ have been listed in Table 2, both in rational and in decimal form. The generator parameter α in this example has been carefully chosen with the first six terms alternating between 1 and 8 and the second six terms constant and equal to 2. This choice allows us to show the interesting property demonstrated in Eq. (47): the Fourier intensities locally behave according to the pattern of the sequence $\{a_j\}_{j=1}^n$. Indeed,

	σ_0	σ_1	σ_2	σ_3	σ_4	σ_5
Rational form, $c_{\nu+1}/c_\nu$	$\frac{140078}{155819}$	$\frac{15741}{140078}$	$\frac{14150}{15741}$	$\frac{1591}{14150}$	$\frac{1422}{1591}$	$\frac{169}{1422}$
Decimal form, σ_ν	0.8989	0.1124	0.8989	0.1124	0.8928	0.1188
	σ_6	σ_7	σ_8	σ_9	σ_{10}	σ_{11}
Rational form, $c_{\nu+1}/c_\nu$	$\frac{70}{169}$	$\frac{29}{70}$	$\frac{12}{29}$	$\frac{5}{12}$	$\frac{2}{5}$	$\frac{1}{2}$
Decimal form, σ_ν	0.4142	0.4143	0.4138	0.4167	0.4000	0.5000

Table 2: Values of the parameter $\sigma_\nu = c_{\nu+1}/c_\nu$, for $0 \leq \nu \leq 11$ both in rational and decimal form, obtained from the continued fraction $\alpha = [0; 1, 8, 1, 8, 1, 8, 2, 2, 2, 2, 2, 2]$. The last value for $n = 12$ is $\sigma_{12} = 0$

the sequence of dominant wavenumbers is obtained from the values σ_ν listed in Table 2. Thus, the first of them (ordered from highest to lowest are)

$$k_1 = 0.8989 k_0, \quad k_2 = 0.1124 k_1, \quad k_3 = 0.8989 k_2, \quad k_4 = 0.1124 k_3, \dots \quad (50)$$

It follows that k_0 and k_1 are quite close to each other, but k_1 and k_2 are far apart. These distances between the wavenumbers are the reflection in the reciprocal space of the jumps between the values 1 and 8 in the sequence. On the other hand, when we evaluate the wavenumbers from k_7 onwards we find

$$k_7 = 0.4142 k_6, \quad k_8 = 0.4143 k_7, \quad k_9 = 0.4128 k_8, \quad k_{10} = 0.4167 k_9, \dots \quad (51)$$

i.e., from $\nu \geq 7$, the wavenumbers are equidistant (in logarithmic scale), reflecting the constant behavior of the sequence as $a_7 = a_8 = \dots = 2$. The behavior described here can be clearly seen in the red-colored coordinates of the dominant wavenumbers in Fig. 3.

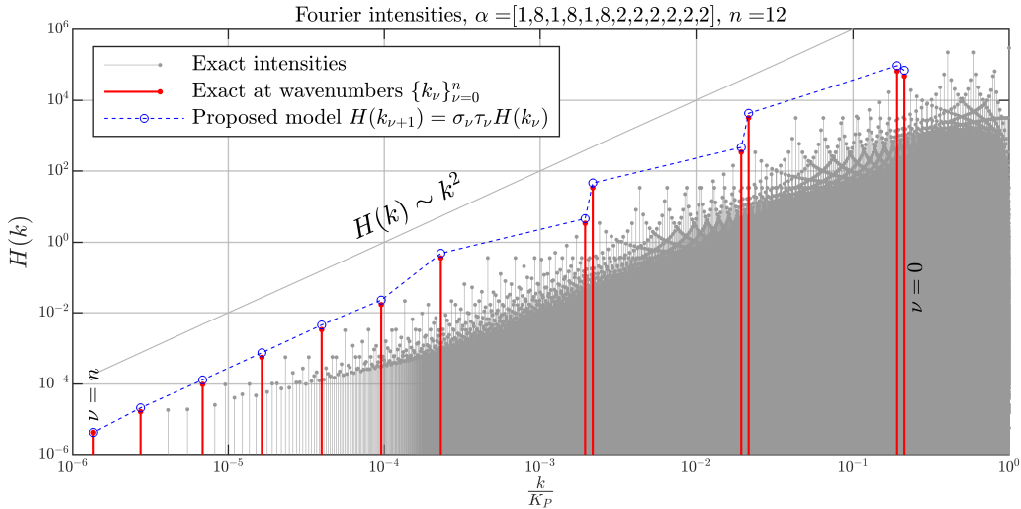


Figure 3: Fourier intensities for a quasiperiodic tiling generated by $\alpha = [0; 1, 8, 1, 8, 1, 8, 2, 2, 2, 2, 2, 2]$. In red color: intensities at the wavenumbers of the dominant sequence $k_\nu = 2\pi c_\nu/L$, $0 \leq \nu \leq n$. In blue color: Proposed model based on density fluctuations

However, if we look at the overall order of decay of the Fourier intensities as $k \rightarrow 0$ in Fig. 3, on average it results very similar to a quadratic law. Let us see in the following sections some results which demonstrate indeed that the quasiperiodic tilings generated by continued fractions are hyperuniform with exponent equal to 3, i.e. $S(k) \sim k^4$. Rigorous proofs will be carried out for the cases of metallic means and for periodic continued fractions. Furthermore, we will prove that for any other system, the order of decay of the structure factor intensities along the whole sequence $\{k_\nu\}_{\nu=0}^n$ is asymptotically a 4th order power law.

5.1. Metallic means: $\alpha = [0; a, a, a, \dots]$

This case collects the behavior of generalized Fibonacci-type quasiperiodic media that could also be simulated using the substitution rule $A \rightarrow B$, $B \rightarrow B^a A$. The order of hyperuniformity has been studied in refs. [2, 3] resulting in a structure factor decaying with the power law $S(k) \sim k^4$, meaning that the Fourier intensities decay strictly quadratically. Let us see that this result can be derived from the model presented in this work. As known [14] the metallic means, represented by the continued fraction $\alpha = [0; a, a, a, \dots]$, are solutions of the quadratic equation $\alpha^2 = 1 + a\alpha$. The two first values of the sequences σ_ν and τ_ν are $\sigma_0 = \alpha$, $\tau_0 = \theta_A/\theta_B$. Since a_j is constant, after several steps σ_ν and τ_ν become approximately equal. Assuming then $n \gg \nu \gg 1$ it yields

$$\sigma_\nu = [0; a, a, \dots] = \alpha \quad , \quad \tau_\nu = [0; a, a, \dots, a + \theta_A/\theta_B] \approx \alpha \quad (52)$$

so that the relationship $H(\sigma_\nu k_\nu) = \sigma_\nu \tau_\nu H(k_\nu)$ can be approximated by

$$H(\alpha k_\nu) = \alpha^2 H(k_\nu) \quad (53)$$

Therefore, the Fourier intensities at the wavenumbers $k = k_\nu$ can be simulated according to the quadratic law $H(k) \sim k^2$ ($k \rightarrow 0$).

It is straightforward that this behavior towards $k \rightarrow 0$ (long wavelength range) is governed by the latest values of sequence $\{a_j\}$ (those with highest values of the index j) which, from the definition of the

sequence $\{k_\nu\}$, are associated to the lowest values of the wavenumbers. Therefore, it is clear that the Fourier intensities will also decay quadratically for tilings generated by continued fractions of the form $\alpha = [0; d_1, \dots, d_m, a, a, a, \dots]$, such as the one shown in Fig. 3. In Fig. 4 (top), both the Fourier intensities and the cumulative function $Z(k)$, defined in Eq. (2), have been represented for the case $\alpha = \sqrt{2} - 1 = [0; 2, 2, 2, \dots]$.

Since $S(k)$ is formed by a set of singular peaks, it should not be induced that the order of the cumulative intensity function is of one order higher. On the contrary, in these cases it turns out that both $S(k)$ and $Z(k)$ share the same exponent [2]. In fact, numerical simulations carried out in this paper shows that, as for the Fibonacci projection cases [2, 3], the scaling of Fourier peaks and their locations produces the cumulative function $Z(k)$ to scale under the same power-exponent as $S(k)$, showing that this property also holds for quasiperiodic tilings generated by continued fractions (see Fig. 4). Therefore, it follows that $Z(k) \sim k^4$, which, according to Eq. (3), immediately leads to an exponent of hyperuniformity $\gamma = 3$. The discrete nature of the spectrum makes the function $Z(k)$ to behave like a cumulative step-wise function as shown in Fig. 4(right).

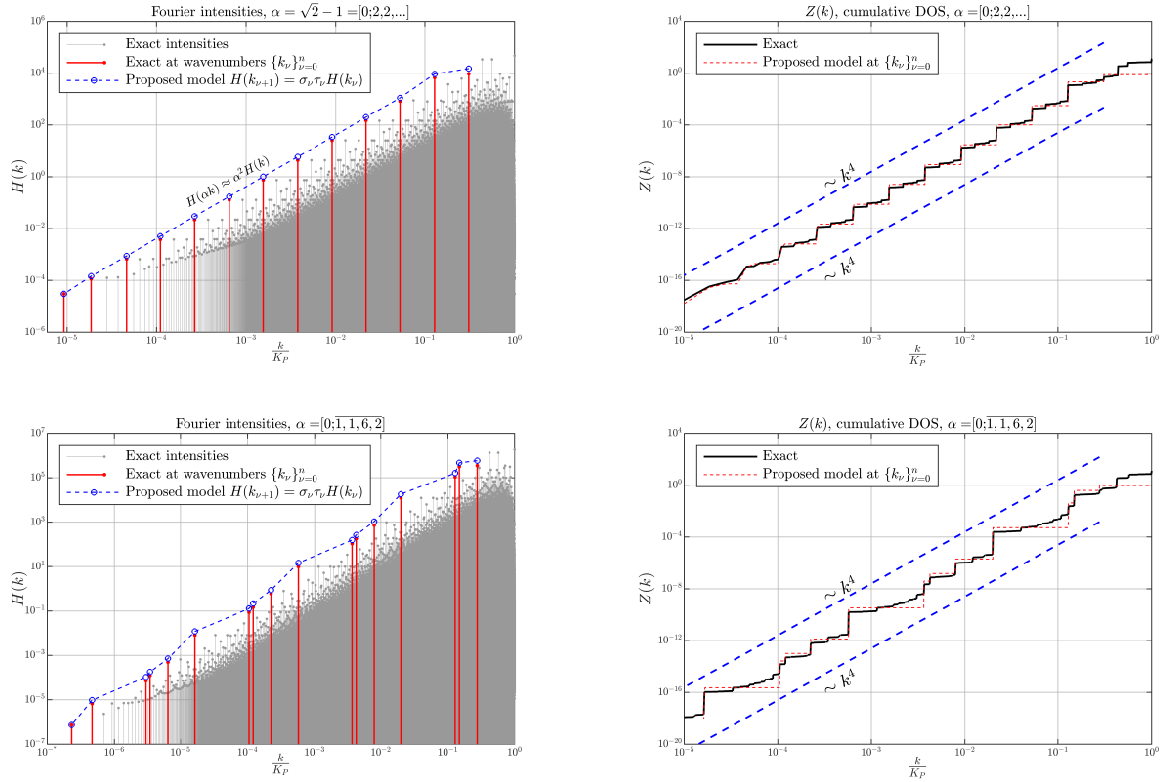


Figure 4: Fourier intensities (left) and cumulative intensity function (right) for two quasiperiodic tilings generated by the silver mean $\alpha = \sqrt{2} - 1 = [0; 2, 2, 2, \dots]$ (top) and by the periodic continued fraction $\alpha = [0; 1, 1, 6, 2]$. In left plots: gray peaks represent the exact Fourier intensities at wavenumbers $k = 2\pi m/L$, $m = 0, 1, 2, \dots$, red peaks represent the exact Fourier intensities at dominant wavenumbers $k_\nu = 2\pi c_\nu/L$, defined in Eq. (31), blue dots: Fourier magnitudes at sequence of wavenumbers $\{k_\nu\}$ obtained by the approximate model. In right plots: black line represents the exact cumulative intensity function, red line represents the cumulative function but obtained from the approximated Bragg peaks at the dominant wavenumbers. Blue dashed line represents the 4th power order envelope curves

5.2. Periodic continued fractions: $\alpha = [0; \overline{a_1, \dots, a_p}]$

Fig. 3 shows that the presence of certain repeating pattern in the sequence $\{a_j\}$ makes the Fourier intensities also reveals periodicity as smaller wavenumbers k are considered. Still, the decay rate of the intensities seems to be quadratic globally, although locally they can be either greater or lower than 2. In this section, it will be proved that, indeed, the global decay order of the Fourier intensities for periodic continued fractions of the form $\alpha = [0; \overline{a_1, \dots, a_p}]$ is exactly 2. The overline notation represents repetition, i.e.

$$\alpha = [0; \overline{a_1, \dots, a_p}] = [0; a_1, \dots, a_p, a_1, \dots, a_p, \dots] \quad (54)$$

Considering $n \gg \nu \gg p$, we can introduce the following values

$$\hat{\sigma} = \sigma_{\nu+1} \cdot \sigma_{\nu+2} \cdots \sigma_{\nu+p}, \quad \hat{\tau} = \tau_{\nu+1} \cdot \tau_{\nu+2} \cdots \tau_{\nu+p} \quad (55)$$

Since the assumed model is multiplicative for both the Fourier intensities and the sequence $\{k_\nu\}$, the value $\hat{\sigma} = k_{\nu+p+1}/k_{\nu+1}$ represents the global jump between the two wavenumbers $k_{\nu+1}$ and $k_{\nu+p+1}$, separated p steps from each other. Due to the periodicity of the continued fraction, the value of $\hat{\sigma}$ is independent of the value of ν considered. With a sufficiently high value of ν fixed, from $k_{\nu+1}$ onwards, the relationship between the Fourier intensities over p steps is

$$\begin{aligned} H(k_{\nu+p+1}) &= \sigma_{\nu+p} \tau_{\nu+p} H(k_{\nu+p}) \\ &= [\sigma_{\nu+p} \cdots \sigma_{\nu+1}] [\tau_{\nu+p} \cdots \tau_{\nu+1}] H(k_{\nu+1}) = \hat{\sigma} \hat{\tau} H(k_{\nu+1}) \end{aligned} \quad (56)$$

Since the relationship between the wavenumbers is

$$k_{\nu+p+1} = \sigma_{\nu+1} \cdots \sigma_{\nu+p} k_{\nu+1} \equiv \hat{\sigma} k_{\nu+1},$$

we can write that

$$H(\hat{\sigma} k_{\nu+1}) = \hat{\sigma} \hat{\tau} H(k_{\nu+1}) \quad (57)$$

Let us now see that the two values $\hat{\sigma}$ and $\hat{\tau}$ are approximately equal provided that $n \gg \nu \gg 1$, where n represents the total size of the sequence $\{a_j\}$. In fact, in order to achieve this, we will determine both $\hat{\sigma}$ and $\hat{\tau}$ separately, finding for them more compact expressions. From Eq. (29), it is

$$\begin{aligned} \hat{\sigma} &= \sigma_{\nu+1} \cdot \sigma_{\nu+2} \cdots \sigma_{\nu+p} \\ &= \left(-\frac{\xi_{\nu+1}}{\xi_\nu} \right) \left(-\frac{\xi_{\nu+2}}{\xi_{\nu+1}} \right) \cdots \left(-\frac{\xi_{\nu+p}}{\xi_{\nu+p-1}} \right) \\ &= (-1)^p \frac{\xi_{\nu+p}}{\xi_\nu} \end{aligned} \quad (58)$$

Now, since $\hat{\sigma}$ does not depend on ν , we can choose any index ν to obtain its value. In particular, it is of interest to take $\nu = 0$, for which Eq. (58) is found to be $\hat{\sigma} = (-1)^p \xi_p / \xi_0$. Using the expression from Eq. (28), we can calculate ξ_p as

$$\xi_p = v_n v_p \left(\alpha - \frac{u_p}{v_p} \right) \quad (59)$$

where as known $\alpha = u_n/v_n$ and $u_p/v_p = [0; a_1, \dots, a_p]$ denotes the p th convergent. Additionally, $\xi_0 = u_n$, so that the value of $\hat{\sigma}$ can be expressed finally as

$$\hat{\sigma} = (-1)^p \frac{\xi_p}{\xi_0} = (-1)^p \frac{v_n v_p}{u_n} \left(\alpha - \frac{u_p}{v_p} \right) = (-1)^p \left(v_p - \frac{u_p}{\alpha} \right) \quad (60)$$

On the other hand, it turns out that the expression for $\hat{\tau}$ given in Eq. (55) can also be meaningfully abbreviated. Each τ_j , $\nu + 1 \leq j \leq \nu + p$ is defined as the ratio between two consecutive tiling lengths, that

is $\tau_j = L_{j-1}/L_j = [0; a_j, a_{j-1}, \dots, a_1 + \theta_A/\theta_B]$, hence they all are finite continued fractions. However, since it is assumed that $\nu \gg p$, then for $\nu + 1 \leq j \leq \nu + p$, τ_j can be approximated as

$$\tau_j = [0; a_j, a_{j-1}, \dots, a_1, a_p, \dots, a_1, \dots, a_p, \dots, a_1 + \theta_A/\theta_B] \approx [0; a_j, a_{j-1}, \dots, a_1, \overline{a_p, \dots, a_1}] \quad (61)$$

where the last expression is an infinite continued fraction. Therefore, the above assumption allow us to write each τ_j as function of the parameter $\beta = [0; \overline{a_p, a_{p-1}, \dots, a_1}]$ obtained from α by reversing the period. Indeed,

$$\begin{aligned} \hat{\tau} &= \tau_{\nu+1} \cdot \tau_{\nu+2} \cdots \tau_{\nu+p} \\ &\approx [0; a_1, \overline{a_p, \dots, a_1}] [0; a_2, a_1, \overline{a_p, \dots, a_1}] \cdots [0; a_{p-1}, \dots, a_1, \overline{a_p, \dots, a_1}] \cdot [0; \overline{a_p, \dots, a_1}] \\ &= \frac{1}{a_1 + \beta} \cdot \frac{1}{a_2 + \frac{1}{a_1 + \beta}} \cdots \frac{1}{a_{p-1} + \frac{1}{a_{p-2} + \frac{1}{\ddots + \frac{1}{a_1 + \beta}}}} \cdot \beta \end{aligned} \quad (62)$$

The above expression shows that $\hat{\tau}$ is constant and independent of ν when considering values $\nu \gg p$ something that will be used later. Using the definition given by $\tau_j = L_{j-1}/L_j$, see Eq. (45), one can simplify the value of $\hat{\tau}$ as

$$\hat{\tau} = \tau_{\nu+1} \cdot \tau_{\nu+2} \cdots \tau_{\nu+p} = \frac{L_\nu}{L_{\nu+1}} \cdot \frac{L_{\nu+1}}{L_{\nu+2}} \cdots \frac{L_{\nu+p-1}}{L_{\nu+p}} = \frac{L_\nu}{L_{\nu+p}} \quad (63)$$

The tilings lengths obey the characteristic recursive sequence $L_j = a_j L_{j-1} + L_{j-2}$ as shown in Eq. (10). Since, as shown above in Eq. (62), $\hat{\tau}$ is independent of ν , we can match the latter with a value ν multiple of the period, i.e., $\nu = mp$, where m is some large natural number. The tiling length in step $\nu + p$ can then be expressed in terms of the lengths of the previous steps up to step L_ν . Following the sequence and using the properties of the corresponding sequences [10], we have

$$\begin{aligned} L_{\nu+p} &= a_p L_{\nu+p-1} + L_{\nu+p-2} \\ &= (a_p a_{p-1} + 1) L_{\nu+p-2} + a_p L_{\nu+p-3} \\ &= (a_p a_{p-1} a_{p-2} + a_{p-2} + a_p) L_{\nu+p-3} + (a_p a_{p-1} + 1) L_{\nu+p-4} = \cdots = \\ &= v_p L_\nu + u_p L_{\nu-1} \end{aligned} \quad (64)$$

where $u_p/v_p = [0; a_1, \dots, a_p]$ is the p -th convergent of α . Dividing by L_ν we obtain finally

$$\frac{L_{\nu+p}}{L_\nu} = u_p \frac{L_{\nu-1}}{L_\nu} + v_p \quad (65)$$

Using again that we are considering $\nu = mp$ as multiple p with $\nu \gg p$, then we can approximate $L_{\nu-1}/L_\nu = \tau_\nu \approx \beta$.

$$\frac{L_{\nu-1}}{L_\nu} = \tau_\nu = [0; a_p, \dots, a_1, a_p, \dots, a_1, \dots, a_p, \dots, a_1 + \theta_A/\theta_B] \approx \beta \quad (66)$$

Plugging Eq. (66) into Eq. (65), the value of $\hat{\tau}$ is finally

$$\hat{\tau} = \frac{1}{v_p + \beta u_p} \quad (67)$$

In order to prove that $\hat{\sigma} \approx \hat{\tau}$, the ratio $\hat{\sigma}/\hat{\tau}$ will be calculated using the derived forms above, (60) y (67).

$$\frac{\hat{\sigma}}{\hat{\tau}} = (-1)^p \left(v_p - \frac{u_p}{\alpha} \right) (v_p + \beta u_p) = (-1)^p \left[v_p^2 - u_p^2 \frac{\beta}{\alpha} + u_p v_p \left(\beta - \frac{1}{\alpha} \right) \right] \quad (68)$$

This expression can be simplified even more making use of a known result concerning periodic continued fractions. Indeed, it can be proved [11] that the following quadratic equation

$$X^2 + \frac{v_p - u_{p-1}}{u_p} X - \frac{v_{p-1}}{u_p} = 0 \quad (69)$$

has $X_1 = \beta$ y $X_2 = -1/\alpha$ as roots. Thus, using the relationships between roots and polynomial coefficients, we have

$$\frac{\beta}{\alpha} = \frac{v_{p-1}}{u_p} \quad , \quad \beta - \frac{1}{\alpha} = -\frac{v_p - u_{p-1}}{u_p} \quad (70)$$

Plugging this result into Eq. (68) and after some algebra it yields

$$\frac{\hat{\sigma}}{\hat{\tau}} = (-1)^p (v_p u_{p-1} - u_p v_{p-1}) = (-1)^p \cdot (-1)^p = 1 \quad (71)$$

where the identity of Eq.(9) has been invoked. Proved the fact that $\hat{\sigma} = \hat{\tau}$, we have finally from Eq. (57) that

$$H(\hat{\sigma} k_{\nu+1}) = \hat{\sigma}^2 H(k_{\nu+1}) \quad (72)$$

which demonstrates the quadratic decay of the Fourier intensities considering the full period of p steps and thus $S(k) \sim k^4$. As above, the fact that the spectrum is formed by a singular set of Bragg peaks makes the cumulative intensities to behave under the same power-law, that is, enveloped as $Z(k) \sim k^4$. Fig. 4(bottom) show the Fourier intensities $H(k)$ and their cumulative function $Z(k)$ for the system generated by the periodic continuous fraction $\alpha = [1, 1, 6, 2]$, with a period of 4 digits. According to theoretical derivations, the Bragg peaks associated with the sequence of dominant wavenumbers $\{k_\nu, 0 \leq \nu n\}$ are also arranged periodically on the logarithmic scale. The Fourier magnitudes are scaled under the same pattern that the density fluctuations every 4 steps, something that is clearly reflected in both plots. It is observed that the power-law enveloping the $Z(k)$ function is exactly of order 4, validating the theoretical pattern derived in Eq. (72).

In the two previous sections the cases of periodic irrational numbers have been considered. The general case of a tiling generated by any continued fraction is studied in the next section, showing that the global asymptotic exponent of the decreasing Fourier intensities towards $k \rightarrow 0$ is demonstrated to be quadratic.

5.3. The general case: $\alpha = [0; a_1, \dots, a_n]$

After studying the specific cases seen in the previous two points, it is worth asking whether the detected behavior can be generalized to any quasiperiodic medium generated by a continued fraction $\alpha = [0; a_1, \dots, a_n]$, exhibiting hyperuniform behavior and a structure factor that tends to zero according to a quartic law, i.e., $S(k) \sim k^4$ as $k \rightarrow 0$. It has been shown that, locally, differences in the values of the sequence $\{a_j\}$ are reflected in perturbations of the Fourier intensities, as observed in the numerical examples in Figs. 2 and 4. Thus, the exponent $1 + \log \tau_\nu / \log \sigma_\nu$, which affects the wavenumbers according to Eq. (47), may have high local values. However, the structure of the parameters τ_ν and σ_ν themselves causes the slopes to be smoothed out somewhat in subsequent steps as the parameter ν progresses between $0 \leq \nu \leq n$. At this point, we will see that indeed the relationship between the Fourier coefficients at the first and last steps, i.e., $\nu = 0$ and $\nu = n$, is approximately quadratic when $n \rightarrow \infty$. That is,

$$\frac{H(k_n)}{H(k_0)} \approx \left(\frac{k_n}{k_0} \right)^x \quad , \quad n \rightarrow \infty \quad (73)$$

Without loss of generality, we will name again

$$\hat{\sigma} = \sigma_0 \sigma_1 \cdots \sigma_{n-1} \quad , \quad \hat{\tau} = \tau_0 \tau_1 \cdots \tau_{n-1} \quad (74)$$

So that

$$\begin{aligned}
k_n &= \sigma_{n-1} k_{n-1} = \cdots = \sigma_{n-1} \cdots \sigma_1 \sigma_0 k_0 \quad , \quad \equiv \hat{\sigma} k_0 \\
H(k_n) &= \sigma_{n-1} \tau_{n-1} H(k_{n-1}) \\
&= (\sigma_{n-1} \cdots \sigma_1 \sigma_0) \cdots (\tau_{n-1} \cdots \tau_1 \tau_0) H(k_0) \\
&\equiv \hat{\sigma} \hat{\tau} H(k_0)
\end{aligned} \tag{75}$$

Using the expressions (29) and (45), the values of $\hat{\sigma}$ and $\hat{\tau}$ can be simplified as

$$\hat{\sigma} = (-1)^n \frac{\xi_{n-1}}{\xi_{-1}} = \frac{1}{v_n} \quad , \quad \hat{\tau} = \frac{L_{-1}}{L_{n-1}} = \frac{A}{L_{n-1}} = \frac{A}{\tau_n L_n} = \frac{1}{\tau_n (\alpha + \theta_A/\theta_B)} \frac{1}{v_n} \tag{76}$$

Thus, we can then calculate the value of χ as

$$\chi = \frac{\log H(k_n) - \log H(k_0)}{\log k_n - \log k_0} = \frac{\log \hat{\sigma} + \log \hat{\tau}}{\log \hat{\sigma}} = 2 + \frac{\log [\tau_n (\alpha + \theta_A/\theta_B)]}{\log v_n} \approx 2 \quad (n \rightarrow \infty) \tag{77}$$

The above expression tends to 2 because the sequence v_n of natural numbers increases indefinitely, while τ_n in general remains as less than unity.

Several numerical examples have been carried out to verify this property, all of them showing a quadratic exponent in the trend toward the long-wavelength range. Three of them are illustrated in Fig. 5, generated with the following irrational numbers and their corresponding continued fractions

$$\begin{aligned}
\alpha &= \frac{e-1}{e+1} = [0; 2, 6, 10, 14, 18, 22, \dots] = 0.4611715 \dots \\
\alpha &= \ln 2 = [0; 1, 2, 3, 1, 6, 3, 1, 1, 2, \dots] = 0.69314718 \dots \\
\alpha &= \frac{1}{\pi} = [0; 3, 7, 15, 1, 292, 1, 1, 1, 2, 1, 3, 1] = 0.31830988 \dots
\end{aligned} \tag{78}$$

Fig. 5 reveals the asymptotic behavior proved in the theoretical derivation. Although there may be significant fluctuations locally, as for example in the case of $1/\pi$, finally on average the hyperuniformity coefficient is common and equal to $\gamma = 3$.

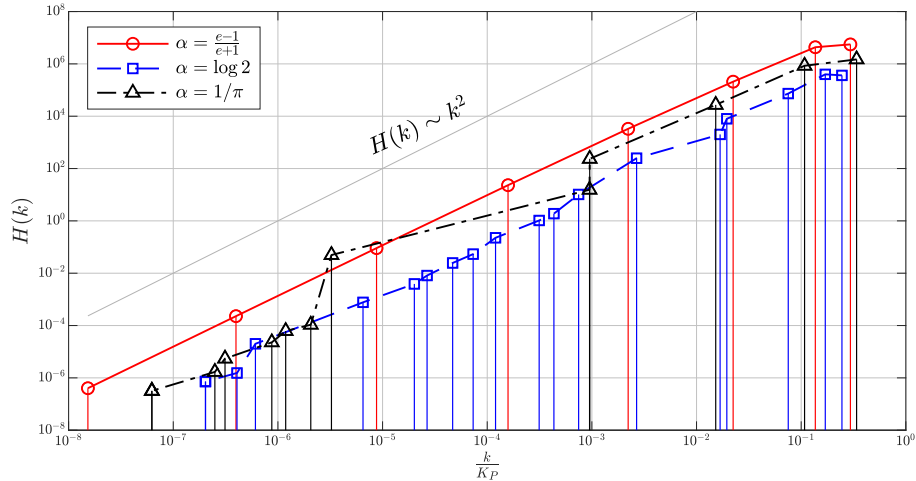


Figure 5: Fourier intensities for three quasiperiodic tilings generated by $\alpha = \{\frac{e-1}{e+1}, \log 2, 1/\pi\}$. The Fourier magnitudes been evaluated at the dominant sequence of wavenumbers, which are no necessarily equal for the three tilings.

6. Conclusions

In this paper the hyperuniformity of one-dimensional quasiperiodic lattices generated by continued fractions has been studied. Given any real number in the interval $[0,1]$ as a continued fraction, we can construct a word or sequence from a binary alphabet, giving rise to quasiperiodic tilings. The studied media are constructed by word concatenation as one-dimensional quasiperiodical distributions of points. The Fourier intensities in the reciprocal space are recursively determined thus exploiting the quasiperiodic nature of the tiling. Among the entire spectrum of Bragg peaks, a sequence of wavenumbers, called *dominant sequence of wavenumbers*, has been identified, showing special properties related to the density fluctuations of the tiling. It has been proved that the pattern of decay of Fourier intensities at this sequence is quadratic regardless the continued fraction, meaning these media are strongly hyperuniform with exponent 3. The theoretical results have been validated and illustrated by means of several numerical examples.

Acknowledgments

Ll. M. García-Raffi and M. Lázaro are grateful for the partial support by the Grant PID2020-112759GB-I00 funded by MCIN/AEI/10.13039/501100011033. M. Lázaro is grateful by the support of the Grant CIGE/2021/141 funded by Generalitat Valenciana (Emerging Research Groups).

References

- [1] S. Torquato, F. H. Stillinger, Local density fluctuations, hyperuniformity, and order metrics, *Phys. Rev. E* 68 (2003) 041113. doi:10.1103/PhysRevE.68.041113.
URL <https://link.aps.org/doi/10.1103/PhysRevE.68.041113>
- [2] E. C. Oğuz, J. E. S. Socolar, P. J. Steinhardt, S. Torquato, Hyperuniformity and anti-hyperuniformity in one-dimensional substitution tilings, *Acta Crystallographica Section A Foundations and Advances* 75 (1) (2019) 3–13. doi:10.1107/s2053273318015528.
- [3] E. C. Oğuz, J. E. S. Socolar, P. J. Steinhardt, S. Torquato, Hyperuniformity of quasicrystals, *Phys. Rev. B* 95 (2017) 054119. doi:10.1103/PhysRevB.95.054119.
- [4] M. Baake, U. Grimm, Diffraction of limit periodic point sets, *Philosophical Magazine* 91 (19-21) (2011) 2661–2670. arXiv:<https://doi.org/10.1080/14786435.2010.508447>, doi:10.1080/14786435.2010.508447.
URL <https://doi.org/10.1080/14786435.2010.508447>
- [5] M. Baake, U. Grimm, Mathematical diffraction of aperiodic structures, *Chem. Soc. Rev.* 41 (2012) 6821–6843.
- [6] C. Godrèche, J. M. Luck, Indexing the diffraction spectrum of a non-pisot self-similar structure, *Phys. Rev. B* 45 (1992) 176–185. doi:10.1103/PhysRevB.45.176.
- [7] J. Luck, C. Godrèche, A. Janner, T. Janssen, The nature of the atomic surfaces of quasiperiodic self-similar structures, *Journal of Physics A: Mathematical and General* 26 (8) (1993) 1951–1999, cited By 86. doi:10.1088/0305-4470/26/8/020.
- [8] J. M. Luck, A classification of critical phenomena on quasi-crystals and other aperiodic structures, *Europhysics Letters (EPL)* 24 (5) (1993) 359–364. doi:10.1209/0295-5075/24/5/007.
- [9] S. Torquato, Hyperuniform states of matter, *Physics Reports* 745 (2018) 1 – 95, hyperuniform States of Matter.
- [10] M. Lázaro, A. Niemczynowicz, A. Siemaszko, L. Garcia-Raffi, Elastodynamical properties of sturmian structured media, *Journal of Sound and Vibration* 715 (2022) Art. 16539. doi:<https://doi.org/10.1016/j.jsv.2021.116539>.
- [11] C. Olds, *Continued Fractions*, Random House (USA), 1963.
- [12] M. Baake, U. Grimm, N. M. nibo, Spectral analysis of a family of binary inflation rules, *Lett Math Phys* 108 (2018) 1783–1805.
- [13] C. Godrèche, J. Luck, Multifractal analysis in reciprocal space and the nature of the fourier transform of self-similar structures, *Journal of Physics A: General Physics* 23 (16) (1990) 3769–3797, cited By 109. doi:10.1088/0305-4470/23/16/024.
- [14] E. Maciá, *Aperiodic Structures in Condensed Matter. Fundamentals and Applications*, Taylor & Francis Group, 2009.